Analyst

Accepted Manuscript

This article can be cited before page numbers have been issued, to do this please use: L. Y. Qin, H. L. Zhang, W. Gong, H. Q. Luo, N. Li and B. L. Li, *Analyst*, 2020, DOI: 10.1039/D0AN01522A.

ROYAL SOCIETY OF CHEMISTRY

rsc.li/analyst

View Article Online
DOI: 10.1039/D0AN01522A

MINIREVIEW

Aggregation-induced responses (AIR) of 2D-derived layered nanostructures enable emerging colorimetric and fluorescence sensors

Received 00th January 20xx,
Accepted 00th January 20xx

DOI: 10.1039/x0xx00000x

Ling Yun Qin,[a] Hong Ling Zhang,[a] Wei Gong,[a] Hong Qun Luo,[a] Nian Bing Li*[a] and Bang Lin Li*[a]

Layered nanostructures (LNs), including two-dimensional nanosheets, nanoflakes, and planar nanodots, own large surface-to-volume ratios, unique optical properties, and desired interfacial activities. It is highly promising that LNs can serve as alternative probes and platforms equipped with numerous merits, e. g. signal amplification, improved recognition, and anti-interference capacities, for emerging sensing applications. Significantly, when the stimuli-responsive aggregation occurs, modified LNs possess the engineered morphologies, attractive optical absorption and fluorescence characteristics, which are remarkably programmable. On the basis of altered aggregation behaviours of LNs, as well as their modulated physical and chemical characteristics, a series of novel sensing assays exhibiting enhanced sensitivity, simple operation, multiple functions, and improved anti-interference capacity are reported, contributing to both the point-of-care testing and high-throughput measurements. Herein, the aggregation-induced response sensing strategies of LNs are comprehensively summarized with the classification of materials and variation of aggregated routes imparting high inspiration in understanding dimension-dependent features, expanding nanoscale biosensor applications, and addressing key issues in disease diagnosis and environmental analysis.

Introduction

The past few decades have seen huge breakthroughs of nanotechnology which remarkably promote nanostructures to be vital elements for sensing.[1-4] Among those nanostructures, gold nanomaterials (NMs) and luminescent semiconducting nanodots (NDs) presented with various morphologies have been largely exploited with dominant roles in fundamental and practical fields, rapidly directing remarkable progresses in bio-targets measurements for disease diagnosis.[5-7] With the scientific development and increasing amount of attention in sensing, the limited characteristics of gold NMs are remarkably exposed.[8-10] For instance, in terms of lateral flow assays, gold NMs are only employed as visual signal providers, but lack of signal amplification function, thereby resulting in the limitation of sensitivity enhancement. Additionally, gold NMs possess highly active surfaces and can be consequently attached with co-existing compounds on material surfaces in biological samples, seriously impeding the reproducibility of gold NMs-based sensing assays.[11-14] Hence, currently, it is urgent to develop alternative nano-probes, which are equipped with unique structures and properties for sensing applications.[15-18]

Inspired by graphene, two-dimensional (2D) materials-derived layered nanostructures (LNs) with the intrinsic features of large planar structures, e. g. layered transition metal dichalcogenides (TMDs), boron nitride, g-C_3N_4, black phosphorus, and planar metal organic frameworks, grow to be rising stars in fields of materials, physics, chemistry, and biomedicine.[19-22] Meanwhile, with the integration of the unique characteristics in fluorescence and optical absorption, LNs with roles of strong surface absorption, desired anti-interferences capacity, and attractive signal readout, could be both signal providers and desired substrates for sensing.[23, 24] Both of the planar structures and unique characteristics change when the aggregation phenomenon of LNs occurs. Significantly, aggregation-based strategies of LNs have contributed to the remarkable progresses in energy storage and conversion,[25-27] electronic devices,[28, 29] stimuli-responsive drug delivery,[30, 31] and environmental protection.[32] Additionally, their aggregation states could also be tailored to achieve signal transformation of photonics and colorimetric features.[33-35] In addition to advantages of the performance, the LNs have relatively large cross-sectional area, while the van der Waals force between the layers is larger and easier to aggregate. Currently, the optical sensing strategies are mainly based on two kinds of signals, which refer to colorimetric and fluorescent responses.[36, 37] Aggregation-induced changes of properties and morphological behaviours mainly lead to the alternation of proton transfer pathways and intensities. Thereby, the readout was exported for target responses with satisfactory results.

[a] School of Chemistry and Chemical Engineering, Southwest University, Chongqing 400715, P. R. China. E-mail: chemlibl@swu.edu.cn; linb@swu.edu.cn

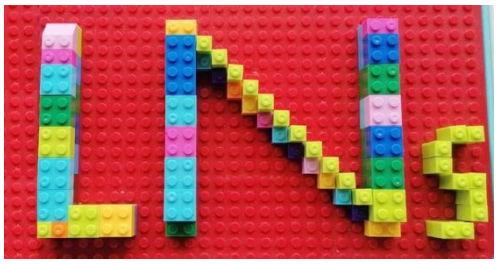

Fig. 1 The scheme showing the stacking of layered "Lego" blocks for building of LNs characters. Significantly, the regular aggregation of LNs induced the colorimetric and fluorescence AIR of targets for construction of emerging sensors.

The changes of optical signals caused by aggregation have been widely used in many fields. On the basis of its simplicity and convenience, scientists continue to improve its accuracy and anti-interference. LNs with intrinsic properties, e. g. large surface-to-volume ratios, modulated bandgaps and steric effects, are challenging the role of classic nano-gold in chem-/bio-sensing, and may become the desired choices for scientists to design aggregation-based sensors. As is shown in Fig. 1, the aggregation model of LNs is similar to the stacking of layered "Lego" blocks, contributing to the construction of desired colorimetric and fluorescence sensors based on both the varied aggregation behaviours and the altered optical properties of LNs. Even though eye-catching achievements have been presented, the associated mechanisms of aggregation-induced responses (AIR) derived from the alternation of intrinsic characteristics are various and widely controversial. Herein, integrated with diverse formats of aggregation, the alternation of features and a deal of sensing strategies are reviewed in great detail and breadth. The principle and applications of the aggregation modules of layered materials for sensing are discussed. Noticeably, this review will inspire readers understand the responsive aggregation strategies of diverse LNs promoting technique-dependent sensing applications, further attract broader attention about AIR alternation, and stimulate superior nanostructures in addressing existing biosensor issues.

Phenomenon of Layered Aggregation

The aggregation behaviours of LNs are discussed, which can be divided into the non-specific and specific coupling aggregation (Fig. 2). The former is mainly attributed to three routes including the van der Waals interaction, strong Π-Π interaction, and electrostatic interaction. Quantitative measurements based on optical mechanisms are thereby established.[38, 39] Additionally, considering that the non-specific aggregation is not directly involved into the target recognition, the integration of other specific processes is essential and thus contribute to the development of emerging sensing assays.[40] In terms of the specific coupling aggregation, target recognition with the output of optical signals is well understood. So far, immunological recognition, DNA complementary pairing, and chemical coupling effects are utilized for exploiting the physical steric changes and properties based on the diversity of LNs types. Meanwhile, among those protocols, LNs

View Article Online
DOI: 10.1039/D0AN01522A

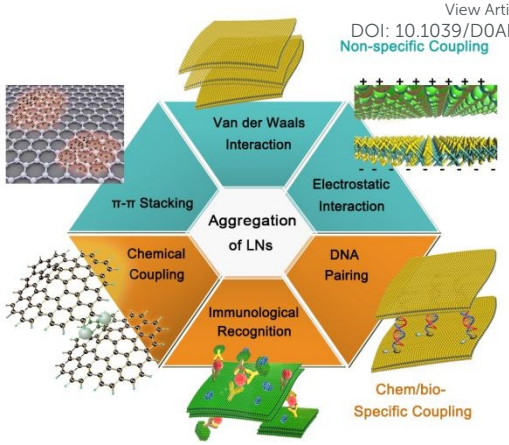

Fig. 2 The scheme indicating the aggregation types of LNs for colorimetric and fluorescence sensors on account of non-specific and specific coupling mechanisms.

are commonly modified with coupling probes which can specifically combine with targets, and thus the stimuli-responsive alternation of LNs subsequently is achieved. Overall, the non-specific aggregation and specific chem/bio-coupling induced aggregation versions of LNs are discussed in detail for directing the construction of fluorescence and colorimetric detection assays.

Non-specific aggregation

In terms of non-specific aggregation model of LNs, it is proposed that electrostatic repulsive potential energy and van der Waals gravitational potential energy exist between colloidal particles as a consequence of the Derjaguin-Landau-Verwey-Overbeek (DLVO) theory, which result in thermodynamics unstable states but dynamics stable states among those particles.[41] On the basis of DLVO theory, the stabilities of LNs could be quantitatively predicted. In principle, the aggregation of nanostructures relys on their surface groups, and environmental conditions in the aggregation unit, such as polarity, ionic strength and pH.[42] For instance, the salt ion can compress the diffusion electric double-layer (EDL) when the electrolyte ion is added into the colloidal solution. Consequently, the higher concentrations of the electrolyte result in the smaller thickness of the diffusion double electric layer. Meanwhile, the electrostatic repulsion potential energy between particles is smaller, and the enhanced gravity makes the colloidal particles agglomerate. Of significance, the Schulze-Hardy rule summarized the relationship between concentrations of salt ions and aggregation behaviours of colloidal particles.[43] The charge number of different ions has a great impact on the deposition of sol. The higher the charge number (valence number) is, the greater the ability of agglomeration is.

Except for electric double-layer (EDL) suppression, heavy metal cations can easily pass through the EDL, attaching on the surface of LNs, and the surface potential of LNs was changed, which promoted to the aggregation of LNs. The electronegativity of the metal cation and the thickness of the hydrated shell discovered that its instability capacity was consistent with its adsorption affinity to LNs.[44] Based on above protocols, two-dimensional (2D) nanostructures achieve

View Article Online
DOI: 10.1039/D0AN01522A

the desired sensing applications for a great deal of targets. For example, NaCl induced aggregation of GO facilitated the determination of trace toxic metal ions by organic solvent-free cloud point extraction.[45] Additionally, the colloidal stability of amphiphilic Janus nanosheets (NSs) and aggregation kinetics were also investigated, which might exhibit high potential in optical sensing applications.[46]

Fig. 3 The sensing properties derived from the aggregation behaviours of LNs determine the diversity of strategies in constructions of emerging colorimetric and fluorescence assays.

Specific coupling aggregation

The properties of colloidal lamellar structure, the deficiency of aggregation behaviours, the lack of specificity and the susceptibility in the solution lead to the lack of reliability in practical analysis. In contrast to non-specific aggregation, stimuli-responsive aggregation occurred according to the specific chemical and biological coupling processes. In that aspect, the functionalization of 2D nanostructure surfaces played a vital role in directing the construction of specific coupling aggregation modules.[47] In order to design a new aggregation mode of materials, scientists functionalized the materials, obtained an emerging aggregation principle and used it for analysis and sensing. In terms of metal ion coupling, the presence of metal ions resulted in the coupling phenomenon, which caused the changes of colorimetric and fluorescence signals for sensing platforms. Additionally, the immunological recognition was usually employed for the vertical aggregation of NSs, where proteins were attached on the layered surfaces, which served as the roles of bio-probes for specific connection.[48, 49] 2D nanostructures are functionalized by proteins, and antigen-antibody specific immunity is used to realize immunoassay. Specific immunological coupling forces promoted to the layered aggregation because of the large surface-to-volume ratios and desired loading capacities of bio-probes.[34] Meanwhile, DNA complementary pairing was a route for specific combination, which contributed to the target-induced aggregation. For instance, Mo *et al*. reported that the ATP-responsive DNA-graphene hybrid nano-aggregates. Li *et al.* reported that DNA complementary pairing could result in the layer-by-layer aggregation of MoS_2 layers with the strong coupling effect of oligonucleotides.[50] Those assays are based on responses of intracellular ATP concentrations which are obviously higher than the extracellular level.[30] Subsequently, DNA-directed self-assembly of GO and magnetic separation was proposed based on strategies of the DNA pairing-induced aggregation.[51]

Aggregated Layer Structures Determine Properties

Understanding the changes of properties when layered aggregation occurred inspired an increasing number of efforts on the exploitation of LNs hosts. Herein, several points were summarized, indicating the progress of aggregation phenomenon of LNs and altered properties based on contributions of colorimetric and fluorescence sensing assays (Fig. 3); 1) Coagulation of aggregated colloidal particles was accelerated by the increasing weights of LNs when the aggregation arose, and the concentration of visual NSs on the supernatant decreased; 2) The steric effects were enhanced due to the aggregation of LNs in the presence of targets, which might be employed for the size-dependent optical sensing assays; 3) The bandgaps of semiconducting NSs were mediated with the aggregation and surface modification. Noticeably, alternation on bandgaps of semiconducting layers would lead to the changes of photonic adsorption, which could be directly recorded on the varied readout of colorimetric signals;[52, 53] 4) The fluorescence quenching phenomenon was attributed to the quantum confinement effects and self-quenching mechanism, where the quantitative measurements of targets via signal-off fluorescence analysis were achieved; 5) The fluorescence quenching phenomenon was attributed to the altered quantum confinement

View Article Online
DOI: 10.1039/D0AN01522A

effects and the self-quenching mechanism, where the quantitative measurements of targets via signal-off fluorescence analysis were achieved; 6) In contrast to the quenching effects, modulation of molecular rotors on specific fluorescent probes resulted in aggregation-induced-emission (AIE) fluorescence enhancement , which exhibited remarkable impacts on optical sensing assays.[54] Additionally, due to the large surface-to-volume ratios, LNs owned huge potential to be desired loading platforms of luminescence dyes, which contributed to the optical sensors.

In terms of LNs, the stimuli-responsive aggregation occurred, which might lead to the alternation of structures and features, as well as the derivation of signals. Subsequently, NMs will settle down considering to the increases of individual weights. With the collection of supernatant, the absorbance of NMs can definitely correspond to the concentration of targets, which followed the Lambert-Beer law. At the same time, the semiconducting LNs own bandgaps, and thus, “naked-eye” observation can identify the aggregation state of layered nanostructures. Firstly, the structure of layered NMs changes, such as the increases of lateral and vertical sizes, which might result in the drops of catalytic site numbers. Additionally, optical signals could be collected from majority of aggregated systems, *e. g.* fluorescence intensity decrease, photonic absorption blue-shift or red-shift. The aggregation phenomenon contributes to the drops of fluorescence intensities and alternation of bandgaps of semiconducting LNs. Additionally, the functionalized LNs could be engineered for expanding the application of stimuli-responsive drug delivery.[55] The prevention from enzyme invasion due to the layered aggregation could not only remarkably enhance the anti-interference effects of enzyme to the nanoarchitectures but also improve the performances of sensing assays.[56]

2D LNs exhibit priority in aggregation assays considering to the large planar structures. Firstly, the large surface-to-volume ratios make 2D nanostructures own desired loading capacitors, promoting to the modification of catching probes and subsequent coupling processes. Secondly, the layered aggregation could contribute to remarkable alternation of intrinsic properties, which create pathway of signal readout and high sensitivity.[57]

Colorimetric Assays

The colorimetric assays based on 2D nanostructures could be divided into two routes. Firstly, the colorimetric imaging with the readout of “naked-eye” observation in either color changes or altered intensities was devoted to chemical and biological measurements. Meanwhile, the colorimetric spectrum analysis definitely contributes to the quantitative measurements of targets with enhanced performances. Overall, LNs exhibited high potential in developing colorimetric assays. Firstly, the LNs could serve as the substrates.[58] Next, LNs equipped with the significant properties can directly offer the colorimetric readout. The intrinsic properties of layered nanostructures accordingly altered with the changes of aggregation phenomenon.

Naked-eye imaging

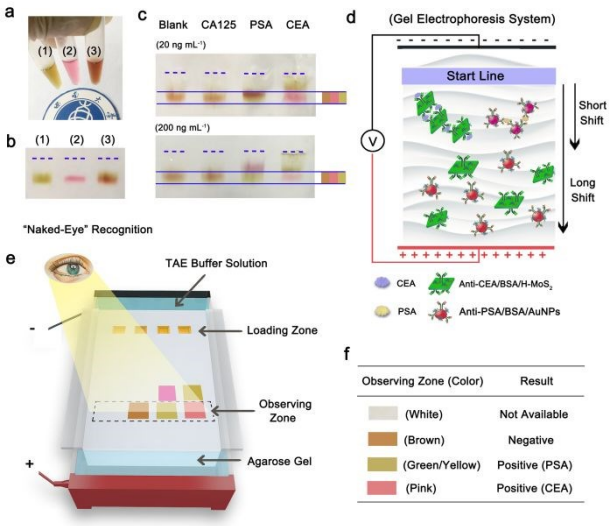

Fig. 4 (a) Pictures of (1) anti-CEA/MoS_2, (2) anti-PSA/AuNPs, and (3) their mixed dispersions, and the corresponding gel electrophoresis images were shown in panel b, respectively. (c) Gel electrophoresis results of mixed nanostructures (anti-CEA/MoS_2 and anti-PSA/ AuNPs) with the addition of diverse proteins, including CA125, PSA, and CEA. (d) The illustration indicating that the migration shifts of anti-CEA/MoS_2 and anti-PSA/AuNPs decreased after the incubation with the specific antigens, respectively. (e) A brief gel electrophoresis assay and (f) a list of colours emerged in the observing zone represent the diverse results, respectively. Reprinted with permission from ref. 35. Copyright 2018, Wiley-VCH.

Integrated with the immunoassay and developed colorimetric probes of LNs (Fig. 4), Li *et al.* reported that 2D TMDs layers with ideal optical properties in aspects of sensing applications were comparable with the classic gold nanoparticles (AuNPs) and the visual measurements of the target carcino-embryonic antigen (CEA) and prostate specific antigen (PSA) were achieved. In that protocol, exfoliated MoS_2 layers and AuNPs were firstly modified with the specific polyclonal antibodies of CEA (anti-CEA) and PSA (anti-PSA) on the surfaces. In the presence of target antigens, layered aggregation of MoS_2 LNs and AuNPs occurred. As an effect of aggregation-induced steric effect, differentiating mobility of antibody-anchored conjugates in gel electrophoresis is a visual response to the specific antigens. Therefore, based on the "naked eye" migration bands in electrophoresis imaging, this study was able to rapidly and simply monitor two kinds of tumour biomarkers using the synergistic probes of antibody-attached layered MoS_2 and AuNPs.[35] It is noted that MoS_2 layers are coupled with catching probes of proteins, performing high stability and anti-interferences in bio-analysis.

Visible absorption spectrometry

Correspondingly, as the lack of absorption of graphene in the visible region, its application in colorimetric analysis is limited. In order to exploit the colorimetric sensing applications of grapheme,

View Article Online
DOI: 10.1039/D0AN01523A

Guo *et al.* prepared the hemin attached graphene NSs and demonstrated that hemin-graphene hybrid NSs (H-GNs) aggregated in electrolyte solution as the consequence of van der Waals interaction and EDL repulsion, which followed the Schulze-Hardy rule. Obviously, the single-stranded DNA (ss-DNA) could strong adsorb on the graphene surfaces via the π-π interaction, whereas the base pairs of double-stranded DNA (ds-DNA) were covered by the negative phosphate backbones which made them away from the negative-charge GO. The H-GNs exhibited recognition ability to ds-DNA and ss-DNA in the optimized electrolyte concentration, considering that ss-DNA and ds-DNA possessed different affinities to the layered NSs. Therefore, an unlabelled colorimetric assay for the detection of hepatitis B virus single nucleotide polymorphisms (SNPs) was established in combination with the coagulation behaviours and peroxidase-like activities of H-GNs.[59] Inspired by the above protocol, Lin *et al.* found that based on the diverse design strategies, protein-mediated aggregation of DNA-hemin-graphene (DNA-GH) complex resulted in the increase or decrease of the colorimetric signal based on the diverse design strategies, achieving the sensing of target protein.[33] Hao *et al.* proposed that DNA pairing could contribute to the layered aggregation between allochroic dyes decorated graphene oxide (GO) and Fe_3O_4 modified GO. When allochroic dyes were employed as signal indicators, the release of dyes was controlled by the pH values and the concentrations of diverse targets could be achieved through the adjustment of the pH of the reaction system.[51]

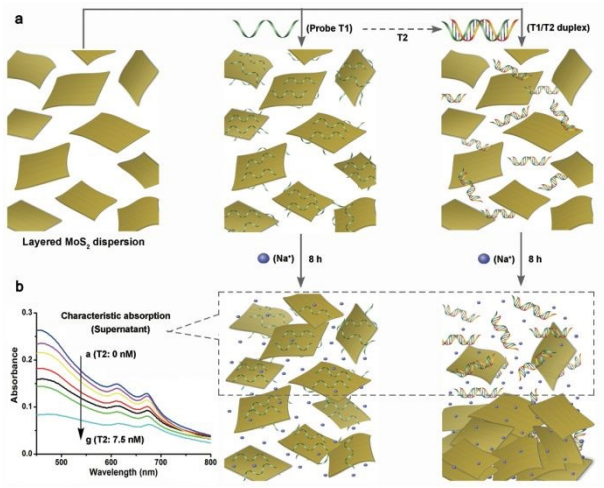

Fig. 5 (a) The illustration of a unlabelled DNA biosensor based on target DNA-induced coagulation phenomenon of layered MoS_2 in aqueous solutions. (b) Absorption spectra of layered MoS_2 with diverse concentrations of target DNA. Reprinted with permission from ref. 60. Copyright 2015, Wiley-VCH.

Additionally, due to the semiconducting characteristics of layered MoS_2, Li *et al.* reported semiconducting MoS_2 layers without the surface modification could be developed as alternative probes of H-GNs in similar colorimetric assays. In that protocol, semiconducting MoS_2 LNs trended to aggregate immediately with the high-concentration salt, resulting in the increases of vertical and lateral sizes of layers. Subsequently, the coagulation of aggregated MoS_2 LNs occurred, resulting in the decrease of characteristic absorption of MoS_2 in the supernatant. Nevertheless, the aggregation phenomenon of MoS_2 layers was hugely inhibited with the prevention of ss-DNA (Fig. 5a). When the ss-DNA probe combined with the target DNA, forming ds-DNA, the DNA hybrids were divorced from MoS_2 surfaces and aggregation of MoS_2 LNs occurred. After the aggregation, layered MoS_2 and DNA hybrids settled down and the characteristic absorbance of supernatant was measured, which could discriminate the ss-DNA and ds-DNA in the MoS_2 system. Therefore, a DNA assay was integrated to achieve the detection of SNPs with features of easy operation and high

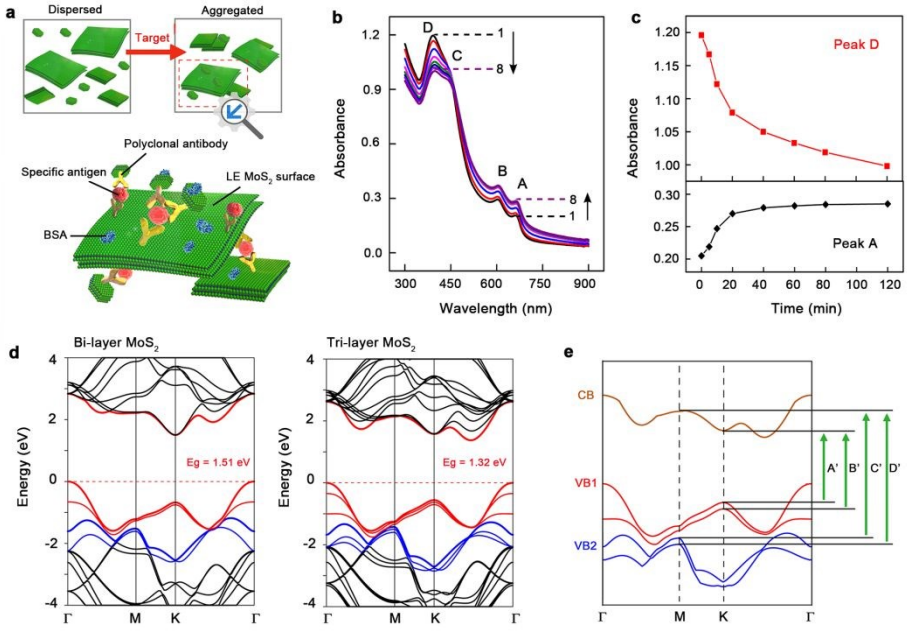

Fig. 6 (a) Illustration of the target-induced aggregated strategy for the novel immunological assay. (b) Optical absorption spectra of anti-CEA modified MoS_2 before (1) and after the addition of CEA for diverse incubation times (2-8: 5, 10, 20, 40, 60, 80, and 120 min). (c) The time-dependent absorbance of peak A and peak D collected from panel b. (d) Electronic bands of bi-layer MoS_2 and tri-layer MoS_2. (d) Schematic illustration indicating the electron transitions of 2D nanostructures. Reprinted with permission from ref. 34. Copyright 2019, Royal Society of Chemistry.

specificity (Fig. 5b).[60] With the inspiration by above work, Lan *et al.* expanded the DNA-induced aggregation and dispersion strategies of MoS_2 with hairpin DNA structures for ss-DNA target detections.[61] In order to expand the applications, Su et al. functionalized AuNPs on layered MoS_2 and the composites exhibited high absorption ability to the antibody capture. Subsequently, the classic "sandwich" structures were formed in the presence of the target antigen, resulting in the decreases of catalytic activities of composites. The turn-off colorimetric signals could be used for the detection of the target proteins based on the immunoassay.[62]

Due to low sensitivity, interferences of coexisting substances and unstable background noises, the single absorbance signal-out of Au nanoplasmonics may lead to false negative or positive results. To overcome these shortcomings, Li *et al.* demonstrated that liquid-exfoliated MoS_2 nano-semiconductors were potential candidates as ratiometric assays by means of size distribution-dependent synergistic photonic absorption characteristics (Fig. 6).[34] Significantly, ratiometric analysis has a series of advantages in quantitative measurement, such as a direct absorbance read-out, which tremendously enhances reliability and reduces the signal-to-noise ratios. The combinatorial results of transverse plane sizes and sheet thicknesses lead to four different excitations in LE MoS_2, and theoretical and experimental results show. An alternation of the size-modulated photonic characteristics resulted from the aggregation-induced morphological conversion of NDs to larger states in possible sensory exploitation (Fig. 6a). The attractive finding was applied in ratiometric immunoassay combined with traditional antibody-antigen specific recognition. It is proved that the developed sensor can achieve the detection of the tumor related antigen, such as CEA. Target antigen induced the antibody-decorated aggregation of LE MoS_2 results in the changes of photonic absorption performance (Fig. 6b and c). With the integration of immunoassays, semiconducting MoS_2 nanoprobes with antibody modifications can use ratiometric photonic absorption measurements, linearly responding to specific targets of CEA ranging from 5.0 to 180.0 ng mL^{-1}.[34] Furthermore, the MoS_2 LNs showed a powerful coupling between the layers , while their energies depended on the thicknesses of layers. The absorption was originated from the transitions around the *K* point. Derived from the spin-orbit coupling at the *K* point, the computational splitting of the valence band (VB) maximum states is accordance to the separation between A and B absorption peaks. Meanwhile, at the *M* point , from the deep VB to conduction band (CB) of the electronic transitions leads to the high absorption energy ranges of C and D excitons (Fig. 6d-e).

Fluorescence Analysis

According to the varying readout mechanisms of fluorescence signals, the fluorescence analysis routes consisted of aggregation-caused quenching (ACQ), AIE, and fluorescence imaging. From the former two assays, majority of LNs were employed as the sensing probes and the quantitative analysis was achieved based on the intensities of fluorescence signals. In the aspect of fluorescence imaging, the LNs were mainly considered as the sensing substrates, constructing the recognition platforms for quantitative analysis of in-vitro and in-vivo targets.

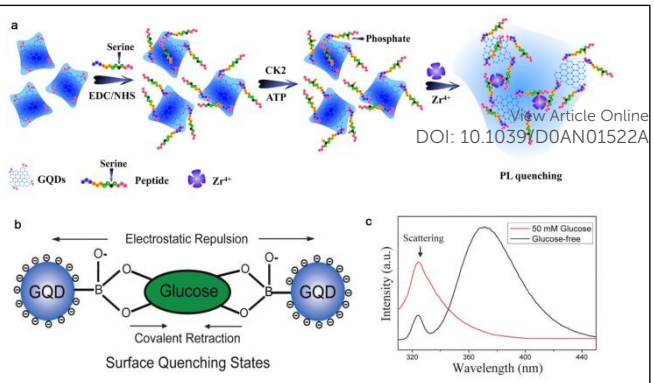

Fig. 7 (a) Scheme illustration of the CK2 kinase assay based on the aggregation of phosphorylated peptide-GQD conjugates through the Zr^{4+} ion linkages. Reprinted with permission from ref. 70. Copyright 2013, American Chemical Society. (b) The mechanism of glucose-induced aggregation of APBA-GQDs. (c) Fluorescent spectra of APBA-GQDs in the presence and absence of glucose. Reprinted with permission from ref. 71. Copyright 2013, Royal Society of Chemistry.

Aggregation-caused quenching

Luminescent dots derived from the planar NSs exhibited superior performance in the sensing application.[63-65] Meanwhile, the fluorescence intensities linearly responsive to the target concentration could be recorded. Due to the quantum confinement effects, graphene quantum dots (GQDs) exhibited desired photoluminescence, which was dependent on the size, surface modification, and element doping.[66-68]

Chen *et al.* prepared pH-sensitive GQDs using one-step hydrothermal procedure, performing a favourable emission transformation at high concentration and in strong acidic media as a consequence of self-assembled J-type aggregation.[69] Wang *et al.* established a simple and sensitive photoluminescence (PL) assay for the activity of a protein kinase by initiating selective aggregation of phosphorylated peptide-GQDs conjugates via the coordination of Zr^{4+} ions (Fig. 7a).[70] In human serum, the inhibition of phosphorylation activity of CK2 by four diverse inhibitors was tested to prove the potential of GQDs-based platform to screen kinase inhibitors in real biological systems. In the presence of inhibitors, the PL intensity increased with the increase of inhibitor efficiency, which is as expected. 3-Aminobenzeneboronic acid (APBA) functionalized GQDs were synthesize, which were utilized as a sensitive and selective sensing platform for glucose (Fig. 7b). Significantly, the protocol successfully achieves the in-vivo glucose monitoring in the striatum of rate, which are integrated with microdialysis. After recognition, APBA groups from negatively charged boronate complexes bound to glucose molecule. Additionally, covalent anchored glucose crosslinking forms APBA-GQDs. The covalent cross-linking and electrostatic repulsion would build a counterbalance of disaggregation and aggregation of the glucose bound APBA-GQDs. The remarkable fluorescence quenching of the surface states were due to the elastic tension introduced by the retractive forces and competing replusive stretching the interface of the GQDs. (Fig. 7c).[71] Zhang *et al.* fabricated MoS_2 QDs with pH-dependent blue fluorescence properties. While at the higher pH, the defect traps of MoS_2 were restored where none of radiation-free recombination is likely to occur, resulting in strong fluorescence. With the increase of

View Article Online
DOI: 10.1039/D0AN01528A

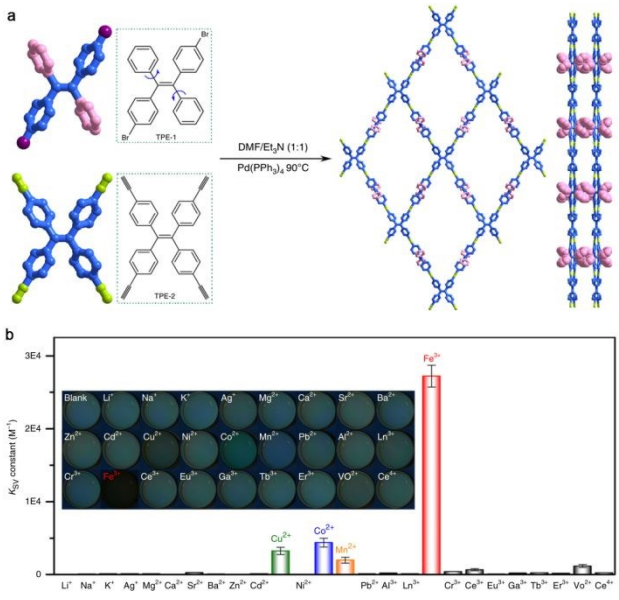

Fig. 8 (a) Synthetic rout of NUS-24 bulk powders. The NUS-24 NSs were obtained from the exfoliation of their bulk powders. (b) The K_{SV} constants of NUS-24 NSs being titrated with different metal ions (left inset: fluorescent photograph of NUS-24 NSs upon titration with different metal ions). Reprinted with permission from ref. 77. Copyright 2017, Nature Publishing Group.

aggregate sizes, the MoS_2 QDs aqueous dispersions showed obvious colour change under acidic condition, ranging from light yellow to dark blue, showing potential application for pH measurements.[72]

In addition to the target-induced aggregation, disaggregation strategies could also be exploited for target recognition. The aggregated GQDs could also be developed as turn-on probes for the fabrication of sensing strategies. Wang et al. utilized aptamer to functionalize GQDs. Significantly, due to the DNA pairing effect, new bioconjugates of aggregated GQDs were formed with the low luminescence intensity. With the incubation of ochrotoxin A (OTA), the aggregation/disaggregation behaviour of GQDs was mediated, resulting in the fluorescence recovery.[73] Based on van der Waals interaction, V_2O_5 nanosheets could strongly adsorb GQDs on their interfaces, and significantly quench the fluorescence. The addition of cysteine contributed to the reduction of V2O5 to V4+ ions, which were accompanied with the release of GQDs and recovery of fluorescence intensity. The developed sensing platform showed linear reponses to cysteine in the wide concentration range.[74]

Aggregation-induced emission

In 2001, Tang *et al.* report an unexpected phenomenon, named as AIE. Firstly, an unusual molecule, 1-methyl-1, 2, 3, 4, 5-pentaphenylsilole, whose isolated species are faintly emissive but whose aggregates are strongly luminescent, was discovered.[75] Significantly, the breakthrough opens the leaf of AIE books with favourable properties and applications.[76] After that, AIE strategies were also demonstrated through the layered aggregation of planar nanostructures. Liu *et al.* prepared photoluminescent carbon dots using tannic acid. When those materials were excited at 350 nm, AIE properties were performed at 455 nm. This phenomenon might be caused by the rotation hindrance of aromatic rings and phenolic hydroxyl group, resulting in exponential decay associated to the permittivity of the solvent.[42] Similar to the AIE mechanism, exposed on the surface of NUS-24 NSs, the dynamic TPE rotors can be restricted in the aggregated state with different water fractions (Fig. 8a), which results in the turn-off detection of Fe^{3+} ions and size-selective turn-on fluorescence by volatile organic compounds (Fig. 8b).[77] Dong *et al.* prepared an all-carbon, 2D π-conjugated aromatic polymer, named NUS-25, containing flexible tetraphenylethylene (TPE) units as aggregation-induced emission molecular rotors. As the partially restricted TPE rotors, NUS-25 NSs have high fluorescence, and can subsequently be used as probes of a chemical sensor to detect acenaphthylene specifically according to quenching mechanism. Significantly, the molecular recognition results from the ultrathin 2D property of NUS-25 NSs, which lead to strong interaction with acenaphthylene and the photoinduced electron transfer behaviour.[78]

A novel AIE sensing strategy based on boron-doped GQDs (BGQDs) was reported by Zhang *et al.*, which could be used for the monitoring of glucose. It was confirmed that BGQDs-glucose aggregates resulted from the reaction of the two boronic acid groups on the BGQDs surfaces with the two cis-diol units in a glucose molecule, which restricts the intra-molecular rotations and contributes to enhancement of PL intensity of fluorescence probes (Fig. 9a).[79] Additionally, Wang *et al.* discovered that Co(II) ions could make the specific aggregation of GQDs, followed by the AIE enhancement. The fluorescence sensing of Co(II) could be developed based GQDs, which owned merits of desired biocompatibility and long-time anti-photo bleaching (Fig. 9b and c). Overall, it showed high potential for in vitro analysis of Co(II) ions.[80] More recently, Zhang *et al.* found a new AIE ligand with great

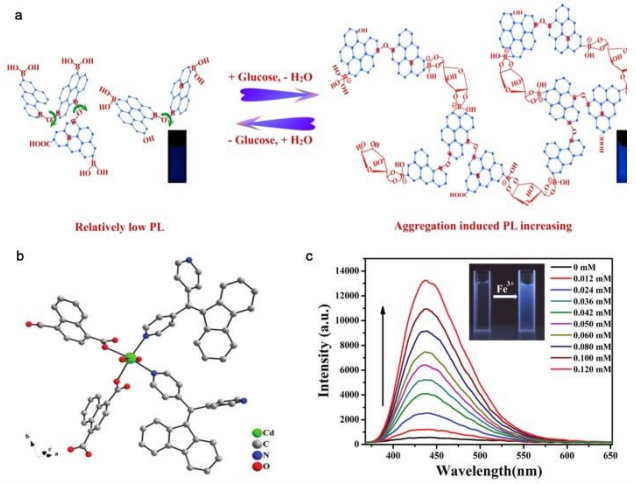

Fig. 9 (a) The mechanism of aggregation-induced PL increases for the glucose-specific sensing by BGQDs. Reprinted with permission from ref. 79. Copyright 2014, American Chemical Society. (b) Coordination environment of the Cd(II) centre in the unit of Cd(II)-organic frame-work. (c) Emission spectra of Cd(II)-organic frame-work dispersed in H_2O with the addition of Fe^{3+} aqueous solution. Reprinted with permission from ref. 80. Copyright 2017, Royal Society of Chemistry.

View Article Online
DOI: 10.1039/D0AN01522A

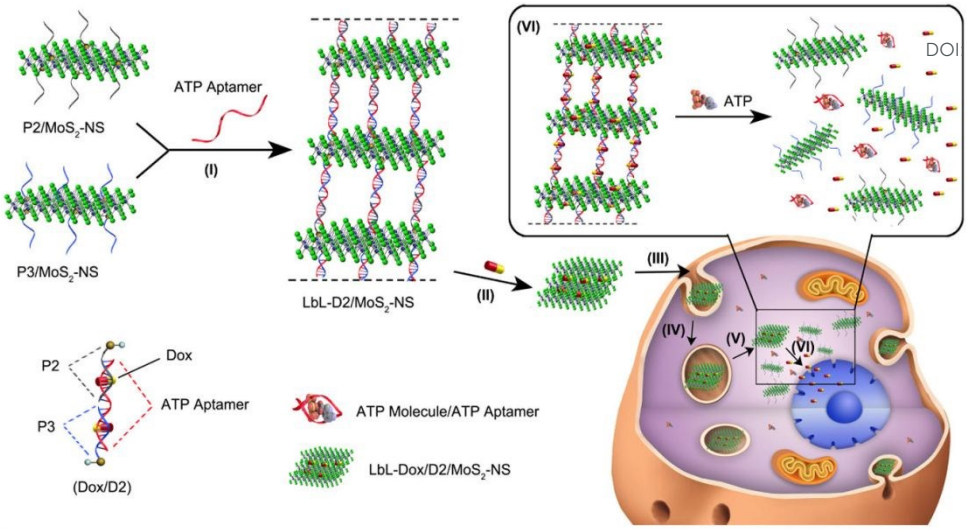

Fig. 10 Schematic illustration of formation of multilayer Dox/D2/MoS_2-NS and the release process of their intracellular Dox. (I) ATP aptamer-induced layer-by-layer (LbL) assembly; (II) Dox loading in multilayer nanostructures; (III) in vitro treatment of Dox/D2/MoS_2-NS; (IV) cell uptake through endocytosis; (V) endosomal/lysosomal escape; (VI) ATP-induced Dox release in the cyotosol for fluorescence imaging. Reprinted with permission from ref. 50. Copyright 2017, American Chemical Society.

stability and excellent luminescence enhancement sensing for Fe^{3+} ions in a water suspension with high sensitivity and selectivity.[81] Compared to other metal ions, the as-synthesized structures are more favourable to form sandwich-like nanoarchitectures with the π-cation-π packing model for Fe^{3+} ions. The phenomenon will significantly improve within the framework of the electron transition, thus increasing the intensity of fluorescence emission.

Fluorescence imaging

LNs could load fluorescence dyes as substrates and fabricate in-vitro imaging assays for the bio-molecular sensing. In those protocols, an ATP-responsive imaging system was developed based on aggregated DNA-graphene cross-linked hybrids. This strategy could be used for recording the cytosol, which owned higher ATP concentrations that the extracellular fluid.[30] Li *et al.* utilized the thiol-labelled DNA to functionalize the MoS_2 LNs (Fig. 10). Subsequently, the DNA pairing-induced layer-by-layer assembly of MoS_2 LNs resulted in the formation of DNA/MoS_2 superstructures, which worked as the carriers of luminescent dyes. DNA hybrids with the cooperation of layered nanoarchitectures could response to ATP level based on intracellular imaging.[50]

Outlook and Horizons

The discriminated performances of LNs-based optical sensing could highly rely on the composition and structures, which might be devoted to the varied features of their intrinsic properties (Table 1). In terms of the composition, LNs could be divided into the inorganic and organic compounds, performing diverse features on establishment of sensors. First of all, the semiconductors of inorganic LNs own modulated bandgaps, resulting in the responsive photonic absorption for target recognition. Additionally, both the planar structures and specific compositions of inorganic LNs promoted the construction of fluorescence-quenching platforms, which were integrated with the different interaction effects for probe assembly. Otherwise, the organic LNs consisting of the layered macromolecules and polymer dots offered comparable characteristics for fluorescence quenching and enhancements for sensing. Furthermore, 2D and 0D nanostructures also exhibited discriminated features in AIR sensing assays. 2D structures served as the alternative colorimetric probes of classic gold nanoparticles

View Article Online
DOI: 10.1039/D0AN01522A

and fluorescence-quenching substrates, whereas the 0D materials mainly offer fluorescence signals for aggregation-induced fluorescence quenching and enhancements routes.

According to the existing works, the aggregation behaviour is not completed in an instant, and the signal change caused by the aggregation will become obvious with the increase of time. The increase of test time may bring some unnecessary variables. Correspondingly, controlling the acceleration of the aggregation speed or designing a rapid aggregation system can reduce the error. Compared with the aggregation in the paper base or the gel, the aggregation in the solution is easily affected by some irrelevant ions, causing errors in actual analysis. Therefore, numerous paper-based sensing and gel sensing systems can be developed.[82-85] In addition, paper-based sensing also has the advantage of simple detection materials and convenient methods, such as pregnancy test bars and HIV test strips that have been developed. No special equipment is needed when the disease diagnosis is conducted. In general, aggregation is irreversible, and only a few cases of aggregation are reversible, such an aggregation-dispersion system can do real-time analysis and observe changes in the target. From the experimental scheme, like ACQ phenomenon, one disadvantage of this aggregation behaviour is that the background signal is high, which reduces accuracy. So we can explore the disaggregation behaviour or AIE system opposite to the aggregation behaviour.

Due to the excavation of emerging characteristics and optimized preparation routes, LNs utilized as desired alternatives of conventional sensing probes, will definitely promote the aggregation-based optical sensors.[86-88] Current drawbacks and merits of those two broads were also listed in this review for a good understanding about the potential and limitations of LNs. The further research topics directing the exploitation of LNs and aggregation-based sensing assays were exhibited. Comparison between conventional Au NPs and MoS_2 NSs in aggregation-based sensing characteristics and applications were exploited for highlighting the synergistic effects. Meanwhile, the toxicity of 2D layered materials is low, thereby exhibiting high potential in in vivo disease diagnosis and therapies.[89-91]

Conclusions

In general, the materials with layered structures will be aggregated by the force or chemical bond between particles, and the aggregation will increase the horizontal and vertical dimensions of

Fig. R1. A summary table indicating the features of LNs-based AIR sensing strategies.

LNs types	Detection systems	Analytes, limit of detection *etc.*	Sensing principles	LNs roles
MoS_2 layers	Visible absorption spectrometry	Target DNA, 0.315× 10^{-9} M;[60] SNPs, single mismatch.[61]	Discriminated coagulation effect.	Substrates for capture, signal providers.
	Gel electrophoresis imaging	CEA, 20 ng mL^{-1}.[35]	Aggregation-induced steric effects.	Naked-eye probes.
	Visible absorption spectrometry	CEA, 5 ng mL^{-1}.[34]	Layer-dependent modulation of bandgaps.	Ratiometric probes.
	Fluorescence imaging	ATP molecules, 0.5 mM.[50]	Disassembly and assembly of layer-by-layer structures.	Substrates for dye loading and quenching.
	Fluorescence spectrometry	pH value, 0.70-3.81.[72]	Aggregation-induced quenching.	Fluorescence providers.
Graphene	Visible absorption spectrometry	SNPs, single base mismatch.[59] Thrombin, 0.5 nM;[33] platelet-derived growth factor, 5 nM.[33]	Artificial enzyme activities.	Substrates for probes.
	Fluorescence spectrometry	Casein kinase II, 0.03 unit mL^{-1};[70] Glucose, 5.0 μM.[71]	Aggregation-induced quenching.	Signal providers, target recognizers.
	Fluorescence spectrometry	Glucose, 0.01 mM;[79] Co^{2+} ions, 2 nM.[80]	Aggregation-induced emission.	Signal providers, target recognizers.
Conjugated polymers	Fluorescence spectrometry	Fe^{3+} ions, 0.9 mM;[77] Acenaphthylene;[78] Fe^{3+} ions, 2.06 mM.[82]	Aggregation-induced emission.	Signal providers, target recognizers.

the material structure, thus changing the zeta potential and hydrodynamic diameter of the material, affecting the electrophoretic mobility and realizing the electrophoretic analysis; the size increase also affects the optical absorption of the material, which can be used for the absorption ratio analysis. The aggregation of materials with fluorescence characteristics can also produce ACQ or AIE, thus opening the application of fluorescence analysis. The signal change caused by aggregation has been widely used in many fields. On the basis of its simplicity and convenience, scientists continue to improve its accuracy and anti-interference. Layered materials with excellent properties are challenging the role of nano-gold in analytical sensing, and may become the first choice for scientists to design aggregation sensors.

The principle and applications of the aggregation modules of LNs for optical sensing were discussed. Noticeably, this review definitely inspire readers understand the responsive aggregation strategies of diverse LNs promoting mechanism-varied sensing applications, further inspire broader attention about variation of aggregation-induced properties and stimulate more attractive nanostructures in addressing existing biosensor issues.

Conflicts of interest

There are no conflicts to declare.

Acknowledgements

We acknowledge the funding provided by the National Natural Science Foundation of China (No. 21675131), the Municipal Science Foundation of Chongqing City (No. CSTC-2015jcyjB50001), and the Fundamental Research Funds for the Central Universities of China (SWU 114089 and XDJK 2014C136). Li B. L. acknowledges the Fundamental Research Funds for the Central Universities of China (SWU 019028) and the Innovation Support Program for Chongqing Overseas Returnees (cx2019086). Li B. L. appreciates his family members, Haolin Zou and Xinye Li, for the cartoon sketch and "Lego" picture, respectively.

Notes and references

1. K. Ariga, X. Jia, J. Song, J. P. Hill, D. T. Leong, Y. Jia and J. Li, *Angew. Chem. Int. Ed.*, 2020, 59, 15424-15446.
2. J. K. Tee, L. X. Yip, E. Tan, S. Santitewagun, A. Prasath, P. C. Ke, H. K. Ho and D. T. Leong, *Chem. Soc. Rev.*, 2019, **48**, 5381-5407.
3. C. Y. Tay, M. I. Setyawati and D. T. Leong, *ACS Nano*, 2017, **11**, 2764-2772.
4. M. Tian, Z. Yuan, Y. Liu, C. Lu, Z. Ye and L. Xiao, *Analyst*, 2020, **145**, 4737-4752.
5. L. Peng, B. L. Li, C. W. Zhou, N. B. Li, M. I. Setyawati and H. L. Zou, *Appl. Mater. Today*, 2018, **11**, 166-188.
6. J. Wang, L. Zhang, F. Peng, X. Shi and D. T. Leong, *Chem. Mater.*, 2018, **30**, 3759-3767.
7. M. I. Setyawati, C. Y. Tay, D. Docter, R. H. Stauber and D. T. Leong, *Chem. Soc. Rev.*, 2015, **44**, 8174-8199.
8. M. I. Setyawati, C. Y. Tay, B. Bay and D. T. Leong, *ACS Nano*, 2017, **11**, 5020-5030.
9. S. Shi, A. Li, R. Huang, J. Yu, S. Li, W. Qi, Z. He and R. Su, *J. Mater. Chem. C*, 2020, **8**, 7552-7560.
10. Y. Wang, Z. Gao, B. Liu and X. Xia, *J. Mater. Chem. C*, 2019, **7**, 15179-15187.
11. K. Zheng, M. I. Setyawati, D. T. Leong and J. Xie, *ACS Nano*, 2017, **11**, 6904-6910.
12. K. Zheng, M. I. Setyawati, D. T. Leong and J. Xie, *Coordin. Chem. Rev.*, 2018, **357**, 1-17.
13. B. Chen, C. Liu, L. Shang, H. Guo, J. Qin, L. Ge, C. J. Jing, C. Feng and K. Hayashi, *J. Mater. Chem. C*, 2020, **8**, 262-269.
14. H. Tan, H. Hu, L. Huang and K. Qian, *Analyst*, 2020, DOI: 10.1039/d0an0057k.
15. Q. Xue, Z. Li, Q. Wang, W. Pan, Y. Chang and X. Duan, *Nanoscale Horiz.*, 2020, **5**, 934-943.
16. P. Yang, S. Zhang, X. Chen, X. Liu, Z. Wang and Y. Li, *Mater. Horiz.*, 2020, **7**, 746-761.
17. Z. Yang, L. Li, A. J. Jin, W. Huang and X. Chen, *Mater. Horiz.*, 2020, **7**, 1474-1494.
18. L. Hu, Z. Xu, F. Long, J. Yuan, H. Li, A. Zhao, S.-T. Han, N. Zhang, X. Liu, C. Ma, S. Ruan and Y.-J. Zeng, *Mater. Horiz.*, 2020, **7**, 1588-1596.
19. B. L. Li, J. Wang, H. L. Zou, S. Garaj, C. T. Lim, J. Xie, N. B. Li and D. T. Leong, *Adv. Funct. Mater.*, 2016, **26**, 7034-7056.
20. H. Zhu, N. Ni, S. Govindarajan, X. Ding and D. T. Leong, *Nanoscale*, 2020, **12**, 43-57.
21. X. Ding, F. Peng, J. Zhou, W. Gong, G. Slaven, K. P. Loh, C. T. Lim and D. T. Leong, *Nat. Commun.*, 2019, **10**, 1-13.
22. F. Peng, M. I. Setyawati, J. K. Tee, X. Ding, J. Wang, M. E. Nga, H. K. Ho and D. T. Leong, *Nat. Nanotech.*, 2019, **14**, 279-286.
23. C. Anichini, W. Czepa, D. Pakulski, A. Aliprandi, A. Ciesielski and P. Samorì, *Chem. Soc. Rev.*, 2018, **47**, 4860-4908.
24. Q. Fan, L. Wang, D. Xu, Y. Duo, J. Gao, L. Zhang, X. Wang, X. Chen, J. Li and H. Zhang, *Nanoscale*, 2020, **12**, 11364-11394.
25. X. Li and L. Zhi, *Chem. Soc. Rev.*, 2018, **47**, 3189-3216.
26. C. Li, Q. Cao, F. Wang, Y. Xiao, Y. Li, J. J. Delaunay and H. Zhu, *Chem. Soc. Rev.*, 2018, **47**, 4981-5037.
27. K. Khan, A. K. Tareen, M. Aslam, Y. Zhang, R. Wang, Z. Ouyang, Z. Gou and H. Zhang, *Nanoscale*, 2019, **11**, 21622-21678.
28. J. Liang, C. Jiang and W. Wu, *Nanoscale*, 2019, **11**, 7041-7061.
29. M. Laipan, J. Yu, R. Zhu, J. Zhu, A. T. Smith, H. He, D. O'Hare and L. Sun, *Mater. Horiz.*, 2020, **7**, 715-745.
30. R. Mo, T. Jiang, W. Sun and Z. Gu, *Biomaterials*, 2015, **50**, 67-74.
31. Jorge Leganés, Ana Sánchez-Migallón, Sonia Merino and E. Vázquez, *Nanoscale*, 2020, **12**, 7072-7081.
32. Q. Yao, S. Wang, W. Shi, C. Lu and G. Liu, *Ind. Eng. Chem. Res.*, 2017, **56**, 583-590.
33. B. Lin, Q. Sun, K. Liu, D. Lu, Y. Fu, Z. Xu and W. Zhang, *Langmuir*, 2014, **30**, 2144-2151.
34. B. L. Li, J. Wang, Z. F. Gao, H. Shi, H. L. Zou, K. Ariga and D. T. Leong, *Mater. Horiz.*, 2019, **6**, 563-570.
35. B. L. Li, L. Y. Peng, H. L. Zou, L. J. Li, H. Q. Luo and N. B. Li, *Small*, 2018, **14**, 1703560.
36. X.-D. Wang and O. S. Wolfbeis, *Chem. Soc. Rev.*, 2014, **43**, 3666-3761.
37. L. Polavarapu, J. Pérez-Juste, Q.-H. Xu and L. M. Liz-Marzán, *J. Mater. Chem. C*, 2014, **2**, 7460-7476.
38. H.-P. Cong, J.-F. Chen and S.-H. Yu, *Chem. Soc. Rev.*, 2014, **43**, 7295-7325.
39. Y. Xu, X. Wang, W. L. Zhang, F. Lv and S. Guo, *Chem. Soc. Rev.*, 2018, **47**, 586-625.
40. S. G. Liu, N. Li, L. Han, L. J. Li, N. B. Li and H. Q. Luo, *Mater. Horiz.*, 2018, **5**, 454-460
41. M. M. Gudarzi, *Langmuir*, 2016, **32**, 5058-5068.
42. Z. X. Liu, Z. L. Wu, M. X. Gao, H. Liu and C. Z. Huang, *Chem. Commun.*, 2016, **52**, 2063-2066.
43. M. Sano, J. Okamura and S. Shinkai, *Langmuir*, 2001, **17**, 7172-7173.
44. K. Yang, B. Chen, X. Zhu and B. Xing, *Environ. Sci. Technol.*, 2016, **50**, 11066-11075.

45. D. Deng, X. Jiang, L. Yang, X. Hou and C. Zheng, *Anal. Chem.*, 2013, **86**, 758-765.
46. T. Yin, Z. Yang, M. Lin, J. Zhang and Z. Dong, *Ind. Eng. Chem. Res.*, 2019, **58**, 4479-4486.
47. G. Guan, S. Zhang, S. Liu, Y. Cai, M. Low, C. P. Teng, I. Y. Phang, Y. Cheng, K. L. Duei, B. M. Srinivasan, Y. Zheng, Y. W. Zhang and M. Y. Han, *J. Am. Chem. Soc.*, 2015, **137**, 6152-6155.
48. D. M. Y. Tay, B. L. Li, E. S. L. Tan, K. P. Loh and D. T. Leong, *Adv. Funct. Mater.*, 2018, **28**, 1801622.
49. J. Zhu, C. Sevencan, M. Zhang, R. S. A. McCoy, X. Ding, J. Ye, J. Xie, K. Ariga, J. Feng, B. H. Bay and D. T. Leong, *ACS Nano*, 2020, **14**, 3259-3271.
50. B. L. Li, M. I. Setyawati, L. Chen, J. Xie, K. Ariga, C.-T. Lim, S. Garaj and D. T. Leong, *ACS Appl. Mater. Interfaces*, 2017, **9**, 15286-15296.
51. N. Hao, J. Lu, Z. Zhou, R. Hua and K. Wang, *ACS Sens.*, 2018, **3**, 2159-2165.
52. B. L. Li, H. L. Zou, J. K. Tian, G. Chen, X. H. Wang, H. Duan, X. L. Li, Y. Shi, J. R. Chen, L. J. Li, J. L. Lei, H. Q. Luo and N. B. Li, *Nano Energy*, 2019, **60**, 689-700.
53. J. Zhu, C. Sevencan, M. Zhang, R. S. A. McCoy, X. Ding, J. Ye, J. Xie, K. Ariga, J. Feng, B. H. Bay and D. T. Leong, *ACS Nano*, 2020, **14**, 3259-3271.
54. C. Tan, X. Qi, X. Huang, J. Yang, B. Zheng, Z. An, R. Chen, J. Wei, B. Z. Tang, W. Huang and H. Zhang, *Adv. Mater.*, 2014, **26**, 1735-1739.
55. B. L. Li, R. Li, H. L. Zou, K. Ariga, N. B. Li and D. T. Leong, *Mater. Horiz.*, 2020, **7**, 455-469.
56. H. Qian, C. Y. Tay, M. I. Setyawati, S. L. Chia, D. S. Lee and D. T. Leong, *Chem. Sci.*, 2017, **8**, 1062-1067.
57. B. L. Li, M. I. Setyawati, H. L. Zou, J. X. Dong, H. Q. Luo, N. B. Li and D. T. Leong, *Small*, 2017, **13**.
58. B. L. Li, H. L. Zou, H. Q. Luo, D. T. Leong and N. B. Li, *Nanoscale*, 2020, **12**, 11979-11985.
59. Y. Guo, L. Deng, J. Li, S. Guo, E. Wang and S. Dong, *ACS Nano*, 2011, **5**, 1282-1290.
60. B. L. Li, H. L. Zou, L. Lu, Y. Yang, J. L. Lei, H. Q. Luo and N. B. Li, *Adv. Funct. Mater.*, 2015, **25**, 3541-3550.
61. L. Lan, Y. Yao, J. Ping and Y. Ying, *Sens. Actuators B: Chem.*, 2019, **290**, 565-572.
62. S. Su, J. Li, Y. Yao, Q. Sun, Q. Zhao, F. Wang, Q. Li, X. Liu and L. Wang, *ACS Appl. Bio Mater.*, 2019, **2**, 292-298.
63. B. L. Li, L. X. Chen, H. L. Zou, J. L. Lei, H. Q. Luo and N. B. Li, *Nanoscale*, 2014, **6**, 9831-9838.
64. H. Cao, W. Dong, T. Wang, W. Shi, C. Fu and Y. Wu, *ACS Sustainable Chem. Eng.*, 2020, **8**, 10939-10946.
65. T. Li, Y. Gao, H. Li, C. Zhang, Y. Xing, M. Jiao, Y. Shi, W. Li, Y. Zhai and Z. Wang, *Analyst*, 2020, **145**, 5206-5212.
66. D. Pan, J. Zhang, Z. Li and M. Wu, *Adv. Mater.*, 2010, **22**, 734-738.
67. W. Li, H. Guo, G. Li, Z. Chi, H. Chen, L. Wang, Y. Liu, K. Chen, M. Le, Y. Han, L. Yin, R. Vajtai, P. M. Ajayan, Y. Weng and M. Wu, *Nanoscale Horiz.*, 2020, **5**, 928-933.
68. K. D. Patel, R. K. Singh and H. W. Kim, *Mater. Horiz.*, 2019, **6**, 434-469.
69. S. Chen, J. W. Liu, M. L. Chen, X. W. Chen and J. H. Wang, *Chem. Commun.*, 2012, **48**, 7637-7639.
70. Y. Wang, L. Zhang, R. P. Liang, J. M. Bai and J. D. Qiu, *Anal. Chem.*, 2013, **85**, 9148-9155.
71. Z. B. Qu, X. Zhou, L. Gu, R. Lan, D. Sun, D. Yu and G. Shi, *Chem. Commun.*, 2013, **49**, 9830-9832.
72. S. Zhang, X. Jia and E. Wang, *Nanoscale*, 2016, **8**, 15152-15157.
73. S. Wang, Y. Zhang, G. Pang, Y. Zhang and S. Guo, *Anal. Chem.,* 2017, **89**, 1704-1709.
74. A. B. Ganganboina, A. D. Chowdhury and R. Doong, *ACS Appl. Mater. Interfaces*, 2018, **10**, 614-624.
75. J. Li, J. Wang, H. Li, N. Song, D. Wang and B. Z. Tang, *Chem. Soc. Rev.*, 2020, **49**, 1144-1172.
76. J. Luo, Z. Xie, J. W. Lam, L. Cheng, H. Chen, C. Qiu, H. S. Kwok, X. Zhan, Y. Liu, D. Zhu and B. Z. Tang, *Chem. Commun.*, 2001, 1740-1741.
77. J. Dong, K. Zhang, X. Li, Y. Qian, H. Zhu, D. Yuan, Q. H. Xu, J. Jiang and D. Zhao, *Nat. Commun.*, 2017, **8**, 1142.
78. J. Dong, X. Li, K. Zhang, Y. Di Yuan, Y. Wang, L. Zhai, G. Liu, D. Yuan, J. Jiang and D. Zhao, *J. Am. Chem. Soc.*, 2018, **140**, 4035-4046.
79. L. Zhang, Z. Y. Zhang, R. P. Liang, Y. H. Li and J. D. Qiu, *Anal. Chem.*, 2014, **86**, 4423-4430.
80. N. Wang, Z. X. Liu, R. S. Li, H. Z. Zhang, C. Z. Huang and J. Wang, *J. Mater. Chem. B*, 2017, **5**, 6394-6399.
81. J. Zhang, S. Ren, H. Xia, W. Jia and C. Zhang, *J. Mater. Chem. C*, 2020, **8**, 1427-1432.
82. S. Shrivastava, T. Q. Trung and N. E. Lee, *Chem. Soc. Rev.*, 2020, **49**, 1812-1866.
83. K. Misawa, T. Yamamoto, Y. Hiruta, H. Yamazaki and D. Citterio, *ACS Sens.*, 2020, **5**, 2076-7085.
84. Z. Chen, Z. Zhang, X. Zhai, Y. Li, L. Lin, H. Zhao, L. Bian, P. Li, L. Yu, Y. Wu and G. Lin, *Anal. Chem.*, 2020, **92**, 7226-7231.
85. F. R. Zhang, J. Y. Lu, Q. F. Yao, Q. Y. Zhu, X. X. Zhang, W. T. Huang, L. Q. Xia, X. Z. Ding, *Analyst*, 2019, **144**, 1881-1891.
86. X. X. Zhang, Q. Y. Zhu, J. Y. Lu, F. R. Zhang, W. T. Huang, X. Z. Ding and L. Q. Xia, *Analyst*, 2019, **144**, 274-283.
87. J. Dong, X. Li, S. B. Peh, Y. D. Yuan, Y. Wang, D. Ji, S. Peng, G. Liu, S. Ying, D. Yuan, J. Jiang, S. Ramakrishna and D. Zhao, *Chem. Mater.*, 2019, **31**, 146-160.
88. Q. Yang, J. Hong, Y. X. Wu, Y. Cao, D. Wu, F. Hu and N. Gan, *ACS Appl. Mater. Interfaces*, 2019, **11**, 41506-41515.
89. E. Tan, B. L. Li, K. Ariga, C. T. Lim, S. Garaj and D. T. Leong, *Bioconjug. Chem.*, 2019, **30**, 2287-2299.
90. L. M. Guiney, X. Wang, T. Xia, A. E. Nel and M. C. Hersam, *ACS Nano*, 2018, **12**, 6360-6377.
91. B. Ma, C. Martín, R. Kurapati and A. Bianco, *Chem. Soc. Rev.*, 2020, DOI: 10.1039/C9CS00822E.

View Article Online
DOI: 10.1039/D0AN01522A

Table of contents

Aggregation-induced responses (AIR) of 2D-derived layered nanostructures enable emerging colorimetric and fluorescence sensors

Ling Yun Qin, Hong Ling Zhang, Wei Gong, Hong Qun Luo, Nian Bing Li and Bang Lin Li**

Target-mediated aggregated states and photonic properties of layered nanostructures (LNs) result in the stimuli-responsive output of colorimetric and fluorescent signals, contributing to the desired construction of emerging chemical and biological sensors.